Supplementary Materials

Gain-of-function mutations in the *phosphatidylserine synthase 1* (*PTDSS1*) gene cause Lenz-Majewski syndrome

Sérgio B Sousa[1,2], Dagan Jenkins[3,18], Estelle Chanudet[4,18], Guergana Tasseva[5,18], Miho Ishida[1], Glenn Anderson[6], James Docker[7], Mina Ryten[8,9], Joaquim Sa[2], Jorge M Saraiva[2,10], Angela Barnicoat[11], Richard Scott[11], Alistair Calder[12], Duangrurdee Wattanasirichaigoon[13], Krystyna Chrzanowska[14], Martina Simandlová[15], Lionel Van Maldergem[16,17], Philip Stanier[7], Philip L Beales[3,4], Jean E Vance[5], Gudrun E Moore[1]

[1]Clinical and Molecular Genetics Unit, UCL Institute of Child Health, London, UK. [2]Serviço de Genética Médica, Hospital Pediátrico, Centro Hospitalar e Universitário de Coimbra, Portugal. [3]Molecular Medicine Unit, UCL Institute of Child Health, London, UK. [4]GOSgene, UCL Institute of Child Health, London, UK. [5]Group on the Molecular and Cell Biology of Lipids, Department of Medicine, University of Alberta, Edmonton, Canada. [6]Histopathology Department, Great Ormond Street Hospital for Children, London. [7]Neural Development Unit, UCL Institute of Child Health, London, UK. [8]Reta Lila Weston Institute, UCL Institute of Neurology, Queen Square, London.[9]Department of Molecular Neuroscience, UCL Institute of Neurology, Queen Square, London. [10]University Clinic of Pediatrics, Faculty of Medicine, University of Coimbra, Portugal. [11]Clinical Genetics Department, Great Ormond Street Hospital, London. [12]Radiology Department, Great Ormond Street Hospital, London, UK. [13]Department of Pediatrics, Faculty of Medicine, Ramathibodi Hospital, Mahidol University, Bangkok, Thailand. [14]Department of Medical Genetics, The Children's Memorial Health Institute, Warsaw, Poland. [15]Department of Biology and Medical Genetics, University Hospital Motol and 2nd Faculty of Medicine, Prague, Czech Republic. [1]Centre de Génétique Humaine, Université de Franche-Comté, Besançon, France. [17]Cutis Laxa Study Group, University of Franche-Comté, Besancon, France. [18]These authors contributed equally to this project. Correspondence should be addressed to S.B.S. (sergio.sousa.09@ucl.ac.uk; sbsousa@chc.min-saude.pt)

Supplementary Table 1 - Clinical features of the five LMS patients included in this study and overall frequency of features in all 10 known typical cases (literature review).

Features	Pat. 1	Pat. 2	Pat. 3	Pat. 4	Pat. 5	Known cases (n=10)
Previous report - reference	New patient	Saraiva 2000[1]	Wattanasirichai-goon et al. 2004[2]	Chrzanowska et al. 1989[3]	New patient	Pat. 1 + Pat. 5 + previous reports[1–10]
Mutation PTDSS1	c.805C>T p.Pro269Ser	c.1058A>G p.Gln353Arg	c.1058A>G p.Gln353Arg	c.1058A>G p.Gln353Arg	c.794T>C p.Leu265Pro	5/5
Confirmed *de novo*	+/+	?/?	+/+	+/+	+/+	4/4
Sex	Male	Female	Female	Male	Female	M=6; F=4
Origin	Kurd-Turkish	Portuguese	Thai-Chinese	Polish	Czech	
Consanguinity	-	-	-	-	-	0/10
Father's age at patient's birth	37	33	35	25	30	34.9 (a)
Mother's age at patient's birth	35	34	31	25	27	
Birth - gestational age (weeks)	38	37	38	41	39	
Length, cm (SD)	?	45 (-1.3)	46 (-1.3)	52 (-1.4)	44 (-4)	3/7 (b)
Weight , g (SD)	2740 (-0.7)	3470 (+1.3)	2100 (<-2)	2550 (-2.5)	2700 (-1.3)	
Head circumference, cm (SD)	?	33 (0)	30 (<-2)	35 (+0.1)	32 (-2.2)	
Post natal growth - age, yrs	2	18	11.5	36	9	
Height, cm (SD)	72.3 (-4)	135 (-4,8)	98 (-7)	128.6 (-7.8)	84 (-10)	10/10 (b)
Weight , kg (SD)	8.2 (-3)	39,5 (-2.9)	17 (-3)	34 (-3.5)	10 (-5)	
Head circumference, cm (SD)	43.3 (-4)	52,5 (-1.6)	50.5 (-2)	53 (-2.7)	44.2(-5)	
Intellectual disability	Mod-Severe	Mild-Moderate	Severe	Borderline	Severe	10/10
Speech impairment	?	+ (sentences)	+++ (absent)	- (good)	++ (2 words)	
Craniofacial features						
Delayed closure of fontanelles	+	+	+	?	+	9/9
Broad/prominent forehead	+	+	+	+	+	10/10
Hypertelorism	+	+	+	+	+	10/10
Large ears	+	+	+	+	+	10/10
Choanal atresia	+	+	?	-	-	7/9
Obstructed nasolacrimal ducts	-	+	+	+	-	7/9
Dental enamel hypoplasia	?	+ (c)	+	+ (c)	+ (c)	8/8
Macroglossia/protruded tongue	+	+	+	-	-	4/8
Macrostomia	+	+	+	+	+	10/10
Prognathism	+	+	+	+	+	7/8
Sparse hair	?	+	+	+	+	5/6

Features	Pat. 1	Pat. 2	Pat. 3	Pat. 4	Pat. 5	Known cases (n=10)
Loose atrophic skin / *cutis laxa*	+	+	+	+	+	10/10
Prominent cutaneous veins	+	+	+	+	+	10/10
Joint laxity	+	+	+	+	+	10/10
Distal limbs						
Brachydactyly, more severe post-axially	+	+	+	+	+	10/10
Proximal symphalangism	+	+	+	+	+	10/10
Cutaneous syndactyly	+	+	+	+	+	10/10
Radiological features						
Skull and vertebra progressive sclerosis	+	+	+	+	+	10/10
Progressive diaphyseal hyperostosis	+	+	- (d)	+	+	8/9
Diaphyseal undermodeling	+	+	- (d)	+	+	8/9
Meta/epiphyseal radiolucency	+	?	- (d)	?	+	6/7
Broad clavicles and ribs	+	+	+	+	+	9/9
Short/absent middle phalanges	+	+	+	+	+	10/10
Phalangeal synostosis	+	+	+	+	+	10/10
Metacarpal synostosis	-	-	-	-	-	1/10
Humero-radial synostosis	-	-	-	+	-	1/10
Hemivertebra + spina bifida oculta	-	-	-	+	-	1/10
Abnormal/delayed skeletal maturation	+	+	+	?	+	9/9
Brain imaging	CT nl at 15m	MRI	CT,MRI,MRV	NP		
Diffuse cortical atrophy		-	+		+	2/3
Hydrocephalus/ enlarged ventricles		-	+		+	3/6
Pituitary hypoplasia		-	+		+	2/3
Leucoencephalopathy		+	+		-	2/3
Small central spinal canal		-	+		-	1/3
Vascular anomalies		-	+ (e)		-	1/3
Dysgenesis of the corpus callosum		+	-		-	1/3
Others						
Cranial nerve palsy	-	-	+	-	-	1/10
Cleft palate	-	-	+	-	-	1/10
Hearing loss	?	+	-	+	-	2/4
Ophthalmological problems	-	Small iris	Entropion	Hypermetropia	-	
Inguinal Hernia	+	+	-	-	-	6/10
Hypospadias and/or chordee	-	NA	NA	-	NA	2/5
Cryptorchidism	+	NA	NA	+	NA	6/6

(a) Mean father's age at birth (yrs) (for 8 of the 10 known patients); (b) patients' length/height <-2SD); (c) all teeth were removed; (d) tubular bones in Pat. 3 show diffuse cortical hyperostosis instead of progressive diaphyseal hyperostosis and metaphyseal radiolucency as typically seen in other LMS patients; (e) persistent fetal origin of the right hypoglossal artery connecting with cervical right internal carotid artery; hypoplasia of straight sinus and accessory falcine sinus; CT – computed tomography; MRI – magnetic resonance imaging; MRV – magnetic resonance venography; + present, - absent; nl – normal. NP – not performed; NA – not applicable.

Remarks on Supplementary Table 1

The father's age at patient's birth was previously suggested to be advanced in LMS patients[4] but this was neither evident in our five cases nor globally in the 10 known cases. The overall mean age was 34.9 yrs; the mean paternal age in the general population is 27; the frequently used criterion for advanced paternal age is >40 yrs[11].

LMS is a progressive condition. With age, bone thickness increases, the radiological characteristics become more severe and the dysmorphic features more evident. The brachydactyly is also progressive, especially at the 4th and 5th rays, with sometimes development of phalangeal and metacarpal synostoses. The height of younger children (aged 3-5 yrs), was approximately -4SD and usually progressed to -7 to -8SD in adulthood. The loose skin might improve with time.

In the five patients in this study, we did not observe significant genotype-phenotype correlations (**Fig. 1** and **Supplementary Table 1**). Pat. 1 and Pat. 5 have the mutations p.Pro269Ser and p.Leu265Pro respectively. The zebrafish studies (**Fig. 5**) suggest that these mutations produce a more severe effect than the p.Gln353Arg mutation. The metabolic studies (**Fig. 3-4**) do not totally support this and clinically, however, it does not appear that Pat. 1 and 5 exhibit a more severe phenotype than Pat. 2, 3 and 4 whom have the p.Gln353Arg mutation. Pat. 2, 3 and 4 share this mutation but also show clear phenotypic differences. For example, Pat. 2 is taller but more severely affected at the craniofacial and intellectual levels than Pat. 4. Pat. 3 has severe intellectual disability as well as cleft palate, cranial nerve palsy and hydrocephalus (not observed in any of the other patients) and his long bones radiological features are somewhat unusual. It is possible that variants in other genes account for this variability.

Besides the 10 known typical LMS patients (8 previously described[1–10] and two patients reported here for the first time), two additional Japanese patients were described with milder phenotypes that overlap considerably with LMS and were proposed to have LMS-like or atypical forms of LMS[12,13]. We think there are significant differences between these two cases and the typical LMS phenotype and we did not include them in the present table. Nevertheless, they might share common pathogenic mechanisms with LMS, being important to screen *PTDSS1* (and eventually other genes involved in phosphatidylserine metabolism) in these patients as well as in other conditions that overlap with LMS, particularly other craniotubular dysplasias without known genetic etiology.

Supplementary Table 2 - Overview of exome sequencing output.

Sample	Yield (kBases)	Reads	Mapped reads	Paired Mapped reads	Mean coverage	% target bases at >=15X	% target bases at >=30X
Pat. 1	9221256	91299584	89669573	87829536	95	89.2	81.1
Father 1	8504384	84201824	82864993	80540344	91	88.9	80.7
Mother 1	8816388	87290972	85753417	83748298	91	88.9	80.9
Pat. 2	8037534	79579552	78277445	76436884	86	88.1	79.4
Pat. 3	8087420	80073476	78231116	75058196	85	88.3	79.5
Pat. 4	7695114	76189260	73960824	67883606	82	87.0	77.4
Father 4	9309552	92173786	89434661	84572100	104	89.1	81.9
Mother 4	9343872	92513596	90221305	86098854	109	90.2	83.8

Supplementary Table 3 – Filtering of variants identified by whole-exome sequencing.

Filtering parameters	Variant filtering			
	Pat. 1	Pat. 2	Pat. 3	Pat. 4
Exonic and splice variants[a]	19,488	19,136	18,970	18,344
Heterozygous	11,631	11,431	10,580	10,676
Nonsense, splice or missense variants	5,618	5,580	5,229	5,151
Novel or rare[b]	406	391	449	274
De novo (trio analysis)	35	NA	NA	26
Predicted damaging[c]	19	195	233	13
	Nº of genes with variants in at least x affected individuals			
		x=2	x=3	x=4
Post above filtering		11	4	1

[a] Included SNV and indels on exons and splice sites (as defined by Ensembl/Polyphen[14]: "a sequence variant in which a change has occurred within the region of the splice site, either within 1-3 bases of the exon or 3-8 bases of the intron")

[b] Included variants that were not present in our internal database containing 80 exomes of phenotypically-characterized individuals processed similarly, and not present in more than 0.5% of the NCBI dbSNP build 132[15] and the 1000Genome[16] databases.

[c] Included nonsense, essential splice-site (as defined by Ensembl/Polyphen[14]: a splice variant that changes the 2 base region at the 5' end or 3' end of an intron) and missense variants predicted damaging by sift[17] and/or polyphen[14]
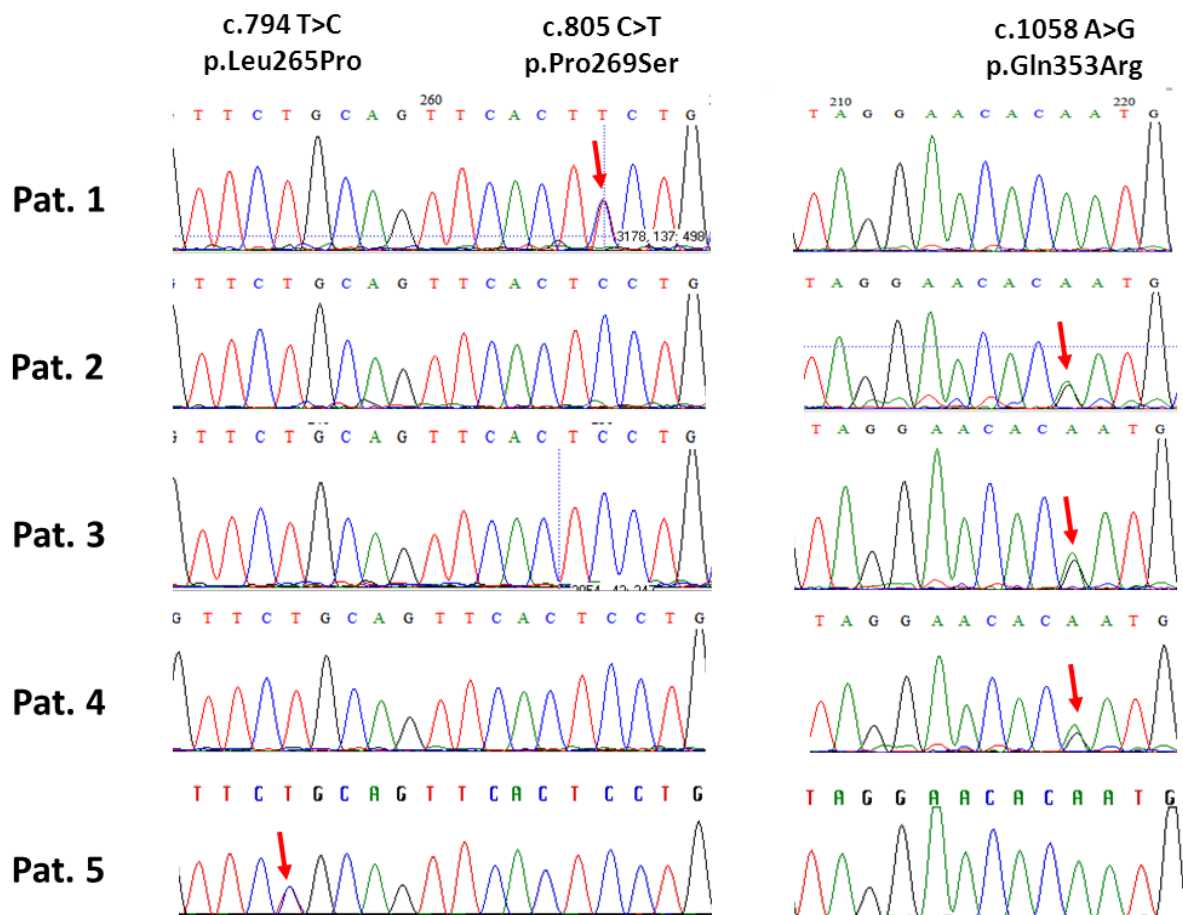
NA – not applicable

Remarks on Supplementary Table 3

The filtering and variant prioritization approach summarized in this table combined data from whole exome-sequencing of both the mother-father-child trios (Pat. 1 and Pat. 4) and the two affected patients (Pat. 2 and Pat. 3) for whom parental DNA samples were unavailable at the time. Considering a *de novo* mode of inheritance within each trio, potentially pathogenic variants were identified in 19 genes for Pat. 1 and 13 genes for Pat. 4. Only 2 genes were common to both affected patients: *PTDSS1* and *MUC17*. The variant identified in *MUC17* in Pat. 4 was paternally inherited but was excluded at the sequence calling level due to insufficient quality and coverage. The analysis of both trios would be sufficient to indicate *PTDSS1* as a single candidate gene.

Supplementary Table 4 – Pathogenicity prediction of the *de novo* missense *PTDSS1* mutations identified in LMS patients using the following *in silico* tools: Polyphen-2[14], PROVEAN[18], SIFT[17] and MutPred[19]. Each mutation was predicted to be deleterious by all programs used.

| Position	Mutation PTDSS1	Polyphen-2[14]	PROVEAN[18]	SIFT[17]	MutPred[19]	
					Probability of deleterious mutation	Molecular Mechanism Disrupted - Top 5 features (P values)
8:97316309	c.T794C p.L265P	Probably Damaging (1.000)	Deleterious (-6.542)	Damaging (0.001)	0.789	Loss of sheet (P = 0.007) Gain of loop (P = 0.024) Gain of disorder (P = 0.0251) Loss of MoRF binding (P = 0.0579) Gain of methylation at K261 (P = 0.0637)
8:97316320	c.C805T p.P269S	Probably Damaging (1.000)	Deleterious (-7.933)	Damaging (0.001)	0.936	Gain of MoRF binding (P = 0.0336) Gain of relative solvent accessibility (P = 0.09) Gain of catalytic residue at P269 (P = 0.1756) Gain of solvent accessibility (P = 0.1846) Gain of sheet (P = 0.1945)
8:97321835	c.A1058G p. Q353R	Probably Damaging (0.999)	Deleterious (-3.488)	Damaging (0.000)	0.828	Gain of sheet (P = 0.039) Loss of ubiquitination at K348 (P = 0.0397) Gain of MoRF binding (P = 0.0534) Gain of relative solvent accessibility (P = 0.1259) Gain of solvent accessibility (P = 0.1319)

Supplementary Figure 1 - Sanger sequencing chromatograms showing the *PTDSS1* heterozygous mutations identified in this study. Patients 2, 3 and 4 share the same missense mutation c.A1058G (p.Gln353Ag) in exon 9. Patients 1 and 5 have point mutations c.C805T (p.Pro269Ser) and c.T794C (p.Leu265Pro), respectively, which are located in exon 7. Position of each mutation is indicated by a red arrow. Sequence analysis of the parents of patients 1, 3, 4 and 5 confirmed these mutations are *de novo* (data not shown).

Supplementary Figure 2 - Clustal W2[20] alignment of the human PSS1 protein and its orthologues in selected species shows a very high degree of conservation. The amino acids residues at each of the identified mutations (Leu265Pro, Pro269Ser and Gln353Ag) are highlighted by grey shaded boxes and are completely conserved.

```
Human        MASCVGSRTLSKDDVNYKMHFRMINEQQVEDITIDFFYRPHTITLLSFTIVSLMYFAFTR 60
Chimpanzee   MASCVGSRTLSKDDVNYKMHFRMINEQQVEDITIDFFYRPHTITLLSFTIVSLMYFAFTR 60
Mouse        MASCVGSRTLSKDDVNYRMHFRMINEQQVEDITIDFFYRPHTITLLSFTIISLMYFAFTR 60
Chicken      MAACVGSRTLSKDDVNYRLHFRMINEQQVEDITLEFFYRPHTITLLSFTILSLMAFAFTR 60
Zebrafish    MATTFRSQTLSKDDVNYRMHFRMINEQQVEDITIQFFYKPHTISLLTVTVLSLMYFAFTR 60
             **:  .  *:*********::************::***:****:**:.*::*** *****

Human        DDSVPEDNIWRGILSVIFFFLIISVLAFPNGPFTRPHPALWRMVFGLSVLYFLFLVFLLF 120
Chimpanzee   DDSVPEDNIWRGILSVIFFFLIISVLAFPNGPFTRPHPALWRMVFGLSVLYFLFLVFLLF 120
Mouse        DDSVPEDNIWRGILSVIFFFLIISVLAFPNGPFTRPHPALWRMVFGLSVLYFLFLVFLLF 120
Chicken      DDSVPEENIWRGILSVIFFFLIISVLAFPNGPFTRPHPAIWRMVFGLSVLYFLFLVFVLF 120
Zebrafish    DDGDPDSNLRVGLILLVSFFLVISVLAFPNGPFTRPHPAIWRIVFGLSVLYFLFLVFIIF 120
             **. *:.*:   *:: :: ***:****************.**:***************:*

Human        LNFEQVKSLMYWLDPNLRYATREADVMEYAVNCHVITWERIISHFDIFAFGHFWGWAMKA 180
Chimpanzee   LNFEQVKSLMYWLDPNLRYATREADVMEYAVNCHVITWERIISHFDIFAFGHFWGWAMKA 180
Mouse        LNFEQVKSLMYWLDPNLRYATREADIMEYAVNCHVITWERIVSHFDIFAFGHFWGWAMKA 180
Chicken      LNFEQVKAVMYWLDPNLRYATREADIMEYAVNCHVITWERILSHFDIFAFGHFWGWAMKA 180
Zebrafish    LNWDQVKALMFWLDPNLRYAKREADVMEYAVNCHVITWERILSHFDIFAFSHFWGWGMKA 180
             **:;***::*:*********.****:****************:********.*****.***

Human        LLIRSYGLCWTISITWELTELFFMHLLPNFAECWWDQVILDILLCNGGGIWLGMVVCRFL 240
Chimpanzee   LLIRSYGLCWTISITWELTELFFMHLLPNFAECWWDQVILDILLCNGGGIWLGMVVCRFL 240
Mouse        LLIRSYGLCWTISITWELTELFFMHLLPNFAECWWDQVILDILLCNGGGIWLGMVVCRFL 240
Chicken      LLIRSYGLCWTISITWELTELFFMHLLPNFAECWWDQVILDILLCNGGGIWLGMVVCRFL 240
Zebrafish    LLIRSYGLCWTISITWELTELFFMHLLPNFAECWWDQVILDILLCNGGGIWLGMTVCRFL 240
             ******************************************************.*****

Human        EMRTYHWASFKDIHTTTGKIKRAVLQFTPASWTYVRWFDPKSSFQRVAGVYLFMIIWQLT 300
Chimpanzee   EMRTYHWASFKDIHTTTGKIKRAVLQFTPASWTYVRWFDPKSSFQRVAGVYLFMIIWQLT 300
Mouse        EMRTYHWASFKDIHTTTGKIKRAVLQFTPASWTYVRWFDPKSSFQRVAGIYLFMIIWQLT 300
Chicken      EMRTYHWASFKDIHTTTGKIKRAVLQFTPASWTYVRWFDPKSSFQRVAGIYLFMIIWQLT 300
Zebrafish    EMRTYHWASIKDIHSTTGKIKRAVLQFTPASWTYVRWLDPKSSLQRVMGVYLFMIIWQLT 300
             *********:*****:*********************:*****:*** *:**********

Human        ELNTFFLKHIFVFQASHPLSWGRILFIGGITAPTVRQYYAYLTDTQCKRVGTQCWVFGVI 360
Chimpanzee   ELNTFFLKHIFVFQASHPLSWGRILFIGGITAPTVRQYYAYLTDTQCKRVGTQCWVFGVI 360
Mouse        ELNTFFLKHIFVFQASHPLSWGRILFIGCITAPTVRQYYAYLTDTQCKRVGTQCWVFGVI 360
Chicken      ELNTFFLKHIFVFQASHPLSWGRILFIGIITAPTVRQYYAYLTDTQCKRVGTQCWVFGVI 360
Zebrafish    ELNTFFLKHIFVFPACHALSWCRILFIGIITAPTVRQYYAYLTDTQCKRVGTQCWVFGAI 360
             ************* *.*.*** ****** *************************.*****.*

Human        GFLEAIVCIKFGQDLFSKTQILYVVLWLLCVAFTTFLCLYGMIWYAEHYGHREKTYSECE 420
Chimpanzee   GFLEAIVCIKFGQDLFSKTQILYVVLWLLCVAFTTFLCLYGMIWYAEHYGHREKTYSECE 420
Mouse        GFLEAIVCIKFGQDLFSKTQILYVMLWLLCVAFTTFLCLYGMVWYAEHYGHREKTYSECE 420
Chicken      AFLEAIVCIKFGQDLFSKTQILYVVFWLLCVAFTTFLCLYGMVWYAEYYGHREKTLSESE 420
Zebrafish    AFLEALACIKFGQDLFSKTQILYVILWLVCLAFITFLCLYVMVWYAENYGPRQKSFSECE 420
             .****:.***************:*:*:** ****** *:**** ** *:*: **:*

Human        DGTYSPEISWHHRKGTKGSEDSPPKHAGNNESHSSRRRNRHSKSKVTNGVGKK 473
Chimpanzee   DGTYSPEISWHHRKGTKGSEDSPPKHAGNNESHSSRRRNRHSKSKVTNGVGKK 473
Mouse        DGTYSPEISWHHGKGSKGSEDSPPKHSSNHESHSSRRRNRHSKSKVTNGVGKK 473
Chicken      DSPYSPDASWLHSKFSKGADNSPPKHPVNSESHSSRRRNRHSRSKVTNGIGKK 473
Zebrafish    DSIYS-------EAGDSVTECKGEFEIDSTTSCSTRKRRDSGDSRTINGMEK- 465
             *. **         . ::  .     .   * *:*:*.  . *:. **: *
```

Supplementary Figure 3 – Specificity of end-product inhibition of phosphatidylserine (PS) synthesis. Control (Ctrl A) and Pat. 4 (Q353R) fibroblasts were seeded at 1.5×10^5 cells/60-mm dishes. After 3 days, cells were incubated in fresh growth medium at 37°C for 2 h in the absence (no add) or presence of phosphatidylcholine (PC) liposomes (80 μM) or PS liposomes (80 μM), then incubated with [3H]serine for 3 h ± PC or PS liposomes. Phospholipids were extracted[21], separated by thin-layer chromatography and radioactivity was measured in PS and PS-derived phosphatidylethanolamine (PE). Note exogenously added PC did not reduce the incorporation of [3H]serine into PS **(a)** or PS-derived PE **(b)** in either Ctrl or LMS fibroblasts. Data are means ± S.D. from triplicate analyses of one of two independent experiments with similar results.
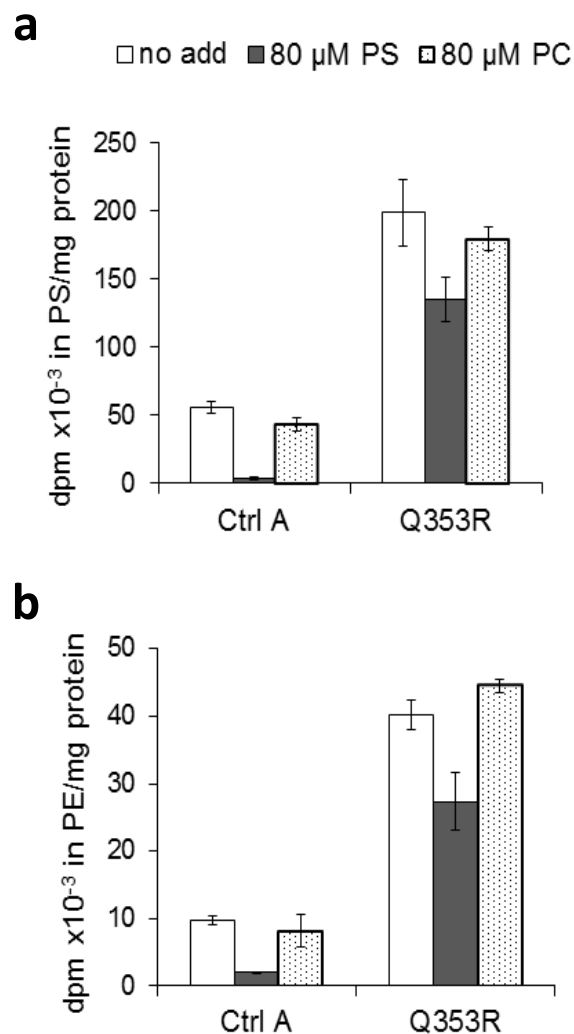
Supplementary Figure 4 - Resistance of serine-exchange activity to inhibition by phosphatidylserine (PS, concentrations 0 to 200 µM) in skin fibroblasts from control (Ctrl) and LMS patients. Serine-exchange activity (PSS1 + PSS2) was measured in the absence (no PS; *white bars*) and presence of indicated amounts of PS liposomes (*grey bars;* 50, 100, or 200 µM PS). In contrast to control cells, in LMS fibroblasts serine-exchange activity was resistant to inhibition by PS, even at the lowest dose used.
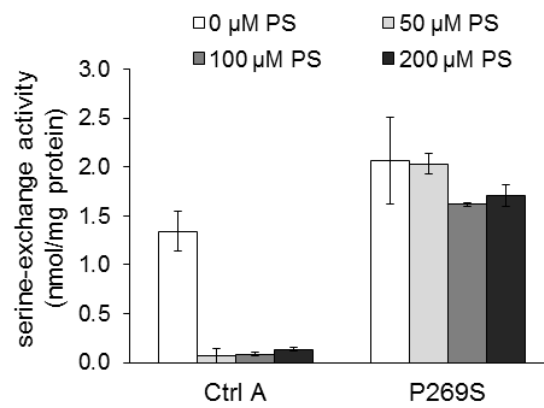
Supplementary Figure 5 – TUNEL staining of zebrafish embryos at 25 hours post-fertilization injected with the highest 500 pg dose of wild-type (WT) or mutant (p.P269S) RNA. Two experiments were performed with >30 injected embryos analyzed in each of them. No difference in apoptosis is observed.

500 pg WT RNA

500 pg WT RNA
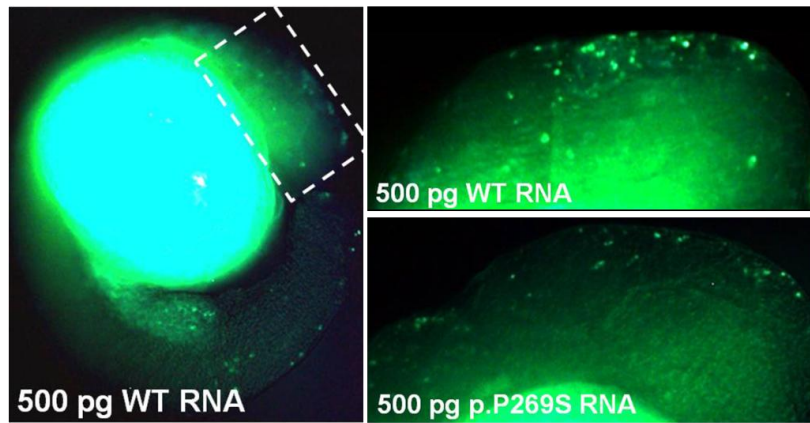
500 pg p.P269S RNA

Supplementary Figure 6 – Anti-phosphohistone H3 staining of zebrafish embryos at 25 hours post-fertilisation injected with the highest 500 pg dose of wild-type (WT) or mutant (p.P269S) RNA compared to an uninjected control. Two experiments were performed with >30 injected embryos analyzed in each of them. No overt difference in cell proliferation (H3+ve cells) was observed.
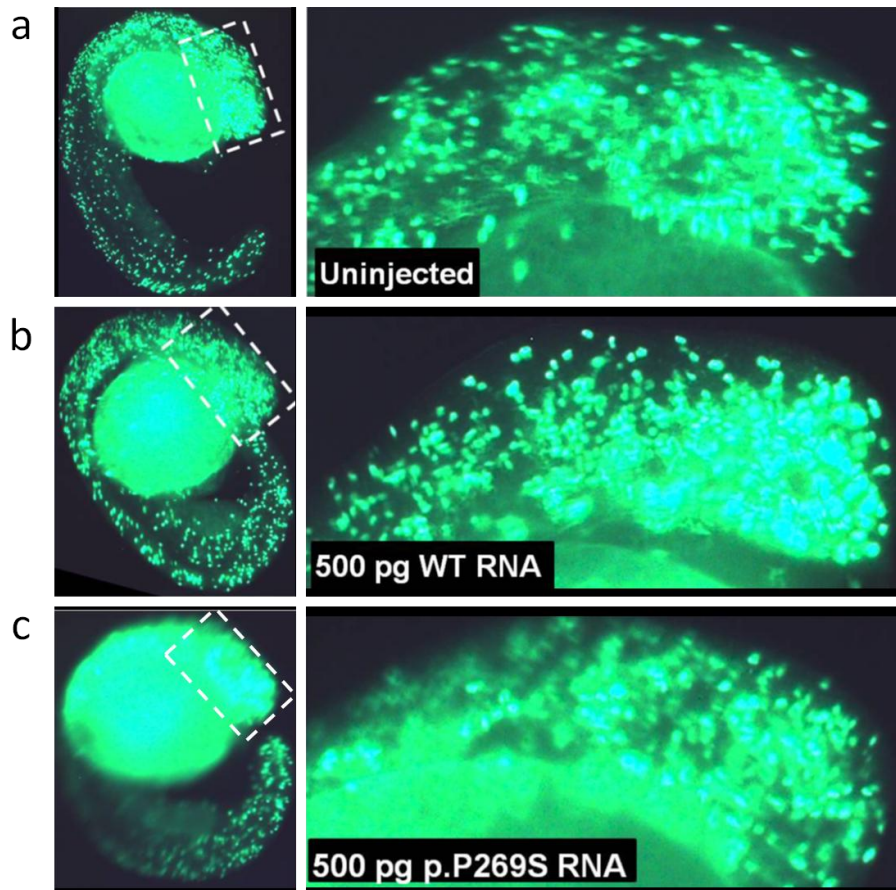
Supplementary Figure 7 – Reverse Transcription Quantitative PCR (RT-qPCR) mRNA analysis of (**a**) *PTDSS1* and (**b**) *PTDSS2* genes in selected tissues from first and second trimester normal human fetuses. mRNA levels for *PTDSS1* and *PTDSS2* are quantified relative to the level of glyceraldehyde-3-phosphate dehydrogenase (GAPDH) mRNA. Data are means ± SEM. N - number of fetuses analyzed for each type of tissue. (**c,d**) Individual results for brain and skin tissues from different fetuses. Note that both brain and skin showed an increasing expression of *PTDSS1* and *PTDSS2* with gestational age during the second trimester of pregnancy.
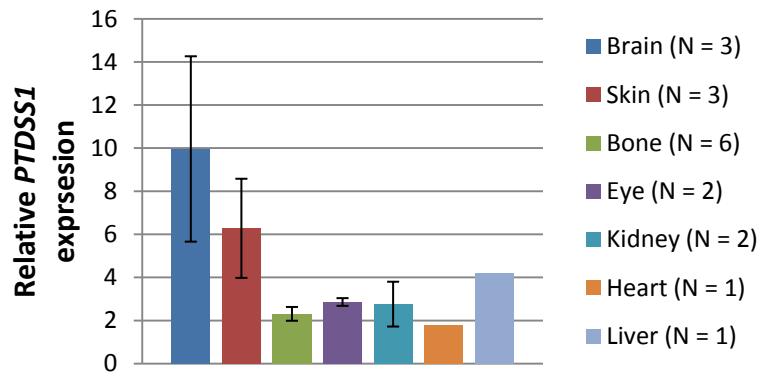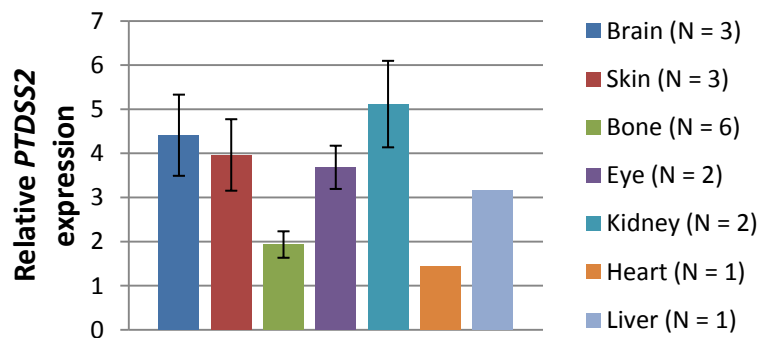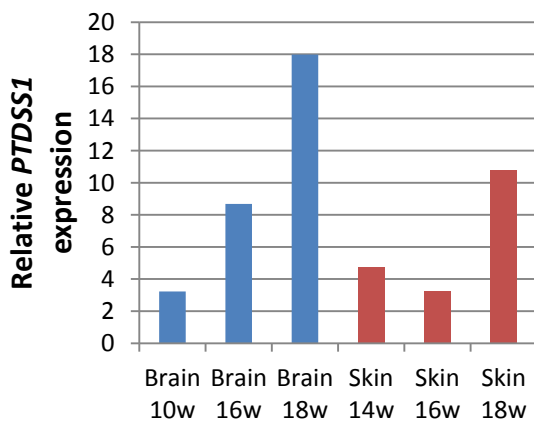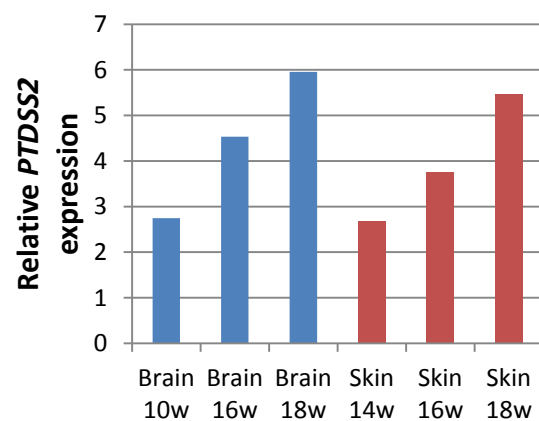
Supplementary Figure 8 - Regional distribution of (**a**) *PTDSS1* and (**b**) *PTDSS2* expression in human brain. Box plots of mRNA levels from 10 brain regions are based on microarray experiments and plotted on a log2 scale (y-axis). Variation in *PTDSS1* and *PTDSS2* transcript expression is shown across 10 brain regions, from left to right: the cerebellum (CRBL, n=130), frontal cortex (FCTX, n=127), hippocampus (HIPP, n=122), medulla (specifically inferior olivary nucleus, MEDU, n=119), occipital cortex (specifically primary visual cortex, OCTX, n=129), putamen (PUTM, n=129), substantia nigra (SNIG, n=101), temporal cortex (TCTX, n=119), thalamus (THAL, n=124), and intralobular white matter (WHMT, n=131). Material and methods were as previously reported[22,23]. In brief, these samples originate from 134 adult individuals from the UK Brain Expression Consortium and were profiled on 1231 Affymetrix Human Exon 1.0 ST arrays. Whiskers extend from the box to 1.5 times the inter-quartile range. (**c-f**) Spatio-temporal *PTDSS1* and *PTDSS2* transcriptome of the human brain using data from the Human Brain Transcriptome (HBT) database[24]. This study assessed 16 brain regions of the brain over 15 periods of the human pre and post-natal development. These data were generated from Affymetrix Human Exon 1.0 ST Arrays performed on 1,340 tissue samples collected from 57 developing and adult post-mortem brains of clinically unremarkable donors representing males and females of multiple ethnicities. (**c,d**) Spatio-temporal expression of PTDSS1 and PTDSS2 mRNA on a log2 scale in 6 brain regions: the cerebellar cortex (CBC), mediodorsal nucleus of the thalamus (MD), striatum (STR), amygdale (AMY), hippocampus (HIP) and the neocortex (NCX). (**e,f**) Spatio-temporal expression of PTDSS1 and PTDSS2 mRNA in 11 regions of the neocortex: 5 at the frontal cortex (OFC, DFC, VFC, MFC, M1C), 2 at the parietal cortex (S1C, IPC), 3 at the temporal cortex (A1C, STC, ITC) and 1 at the occipital cortex (V1C).

a - *PTDSS1*
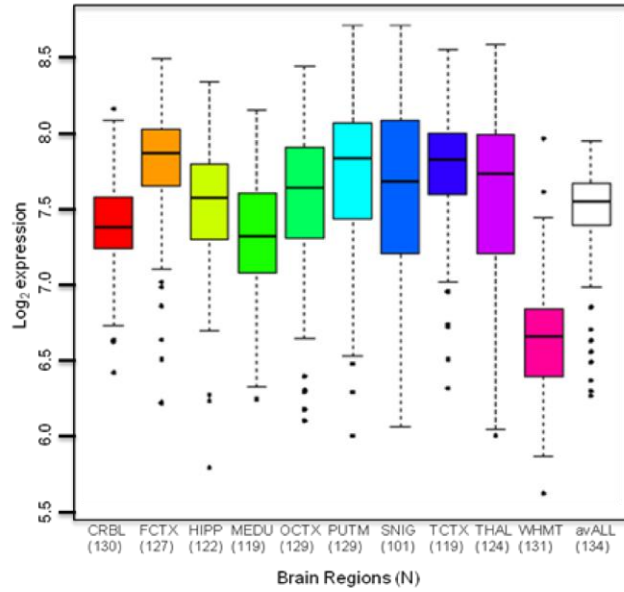
b - *PTDSS2*
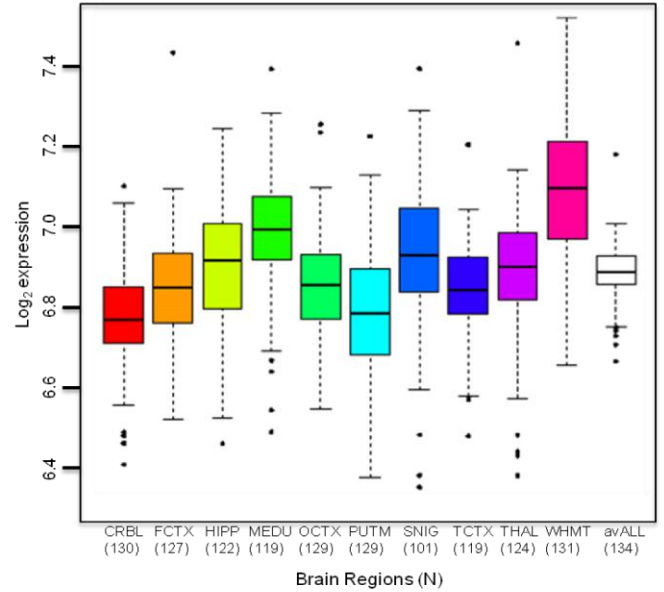
c - *PTDSS1*
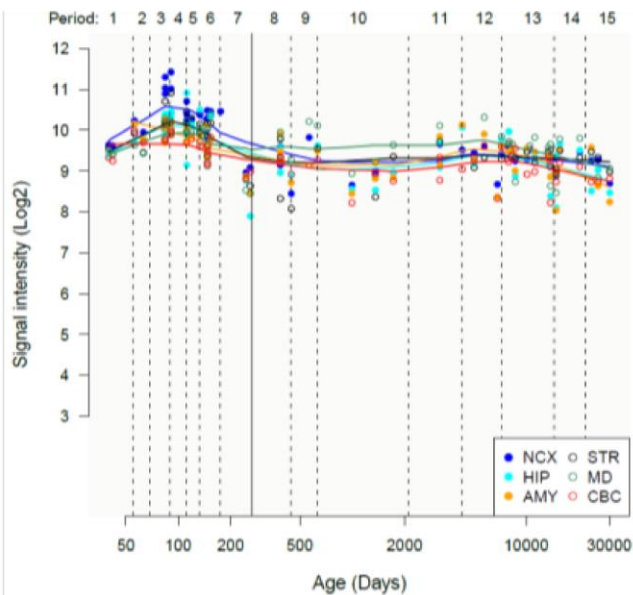
d - *PTDSS2*
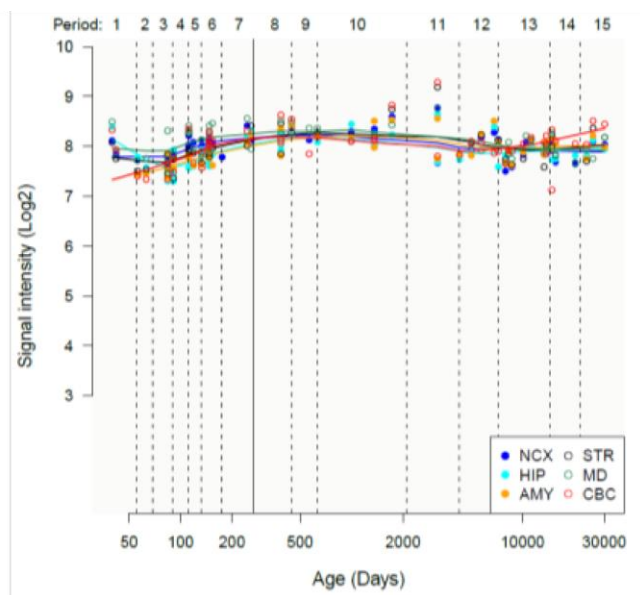
e - *PTDSS1*
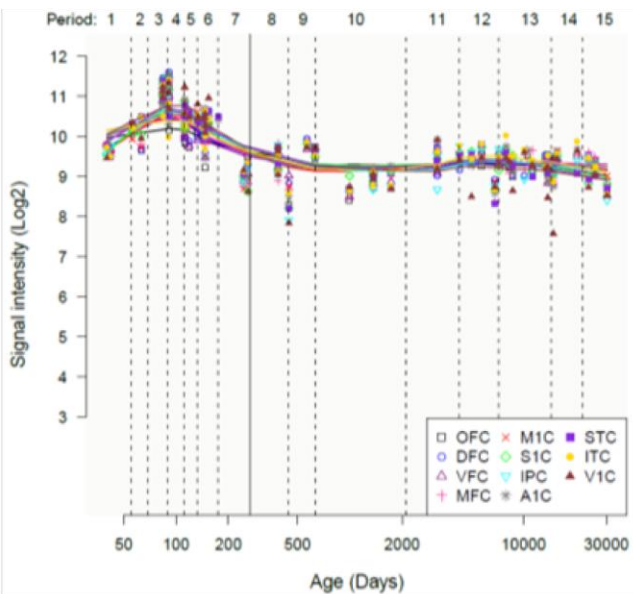
f - *PTDSS2*
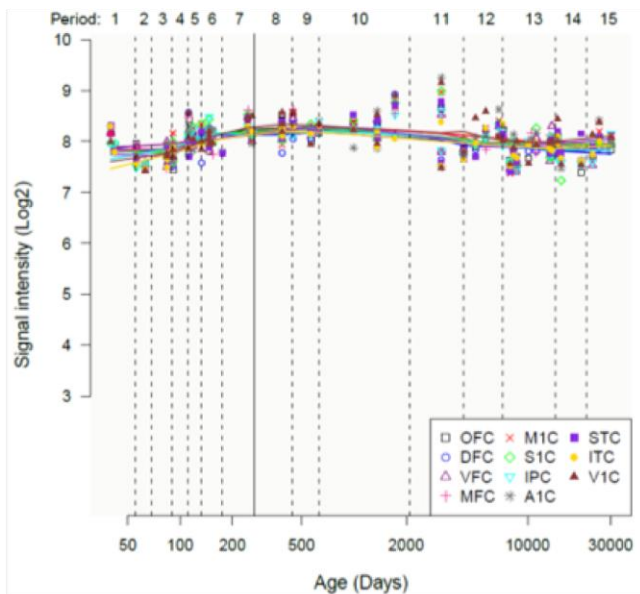
Remarks on Supplementary Figure 8

In these two large sets of data, it is evident the high brain *PTDSS1* and relatively less *PTDSS2* expression. It corresponds to both mouse data and strongly supports our RT-qPCR data from human fetal brain samples (**Supplementary Fig. 6**). The *PTDSS1* expression in the white matter is considerably lower than other regions and relative to the *PTDSS2* profile (**a,b**), while the cerebellum is slightly lower in both array studies (**a,c**). All regions of the neocortex (**e**) show similar high *PTDSS1* expression and some LMS patients do show some degree of cortical brain atrophy. The temporal pattern of *PTDSS1* expression seems consistent in all regions of the brain (**c**) and within the distinct areas of the neocortex (**e**). *PTDSS1* brain expression is significantly higher prenatally showing an evident increase in the first and second trimesters (**c,e**), (corroborating our RT-qPCR results in **Supplementary Fig. 6**), with subsequent decrease in the third trimester but then maintaining high expression throughout childhood and adult life.

Supplementary Figure 9 – Analysis of skin biopsy and cultured fibroblasts using electron microscopy. (**a**) Skin biopsy dermis of Pat. 4 showing two fibroblasts with numerous cytoplasmic vacuoles. There is a paucity of elastic tissue in the surrounding area (original magnification x1200). (**b**) High power view of the tail of a fibroblast from Pat. 4 skin biopsy with membrane bound vacuoles containing granular material suggestive of a degradative or phagocytic process (original magnification x5000). (**c**) Normal skin with fibroblast and grey bands of elastic fibers (arrow), for comparison (original magnification x2000). (**d**) Low power electron micrograph showing a cultured fibroblast from Pat. 1. Note the displaced nucleus and numerous vacuoles with mainly electron dense material (original magnification x1,200). (**e**) High power image of the same cell with membrane bound vacuoles and stored material. The density and morphology of the material is suggestive of having a lipid component (original magnification x4000). Similar findings were observed in cultured fibroblasts from Pat. 4. (**f**) Control cultured fibroblast for comparison. Low power image of control sample showing a solitary fibroblast with empty cytoplasmic vacuoles (original magnification x 1200). (**g**) High power image of the same cell with a few mitochondria, rough endoplasmic reticulum and no stored material in the vacuoles (original magnification x4000).
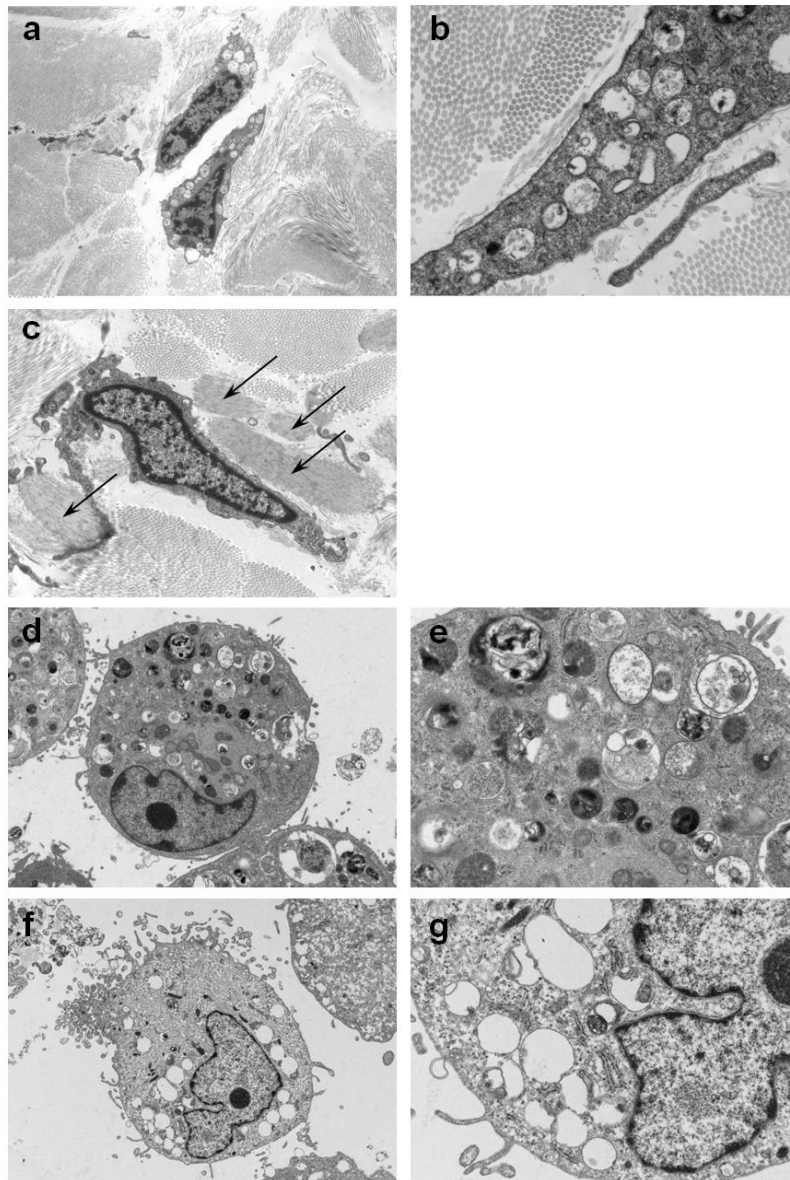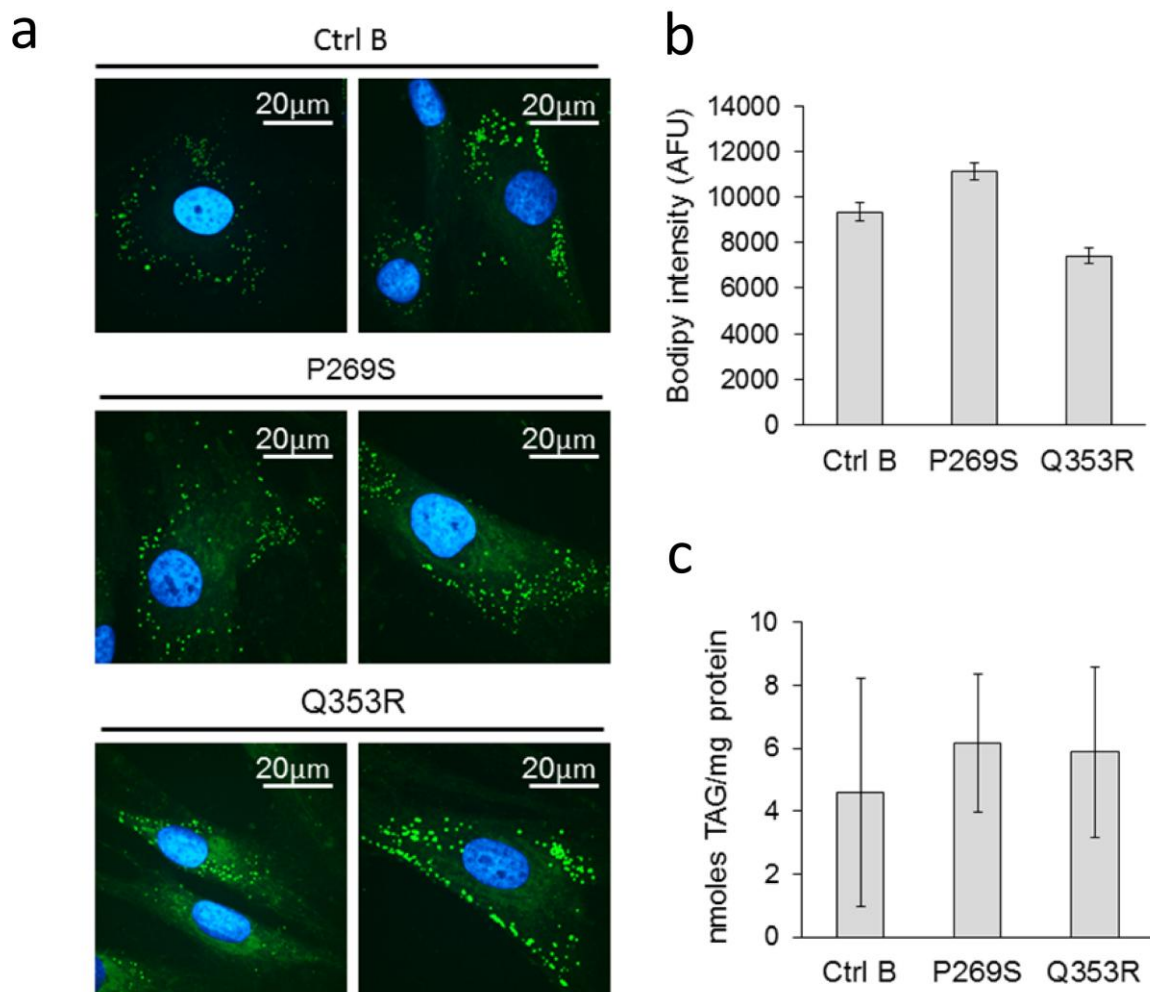
**Remarks on Supplementary Figure 9**

Electron microscopy studies of peripheral blood leucocytes in two of our patients did not reveal any consistent abnormality. Infrequent lymphocytes appear to contain small membrane bound cytoplasmic vacuoles with no specific identifiable material.

We have specifically looked for signs of apoptosis in all the electron microscopy images of skin from Pat. 4, blood lymphocytes and fibroblast cultures from Pat. 1 and Pat. 4 LMS patients. We could not find convincing evidence of true apoptosis in any of the samples.

Supplementary Figure 10 - Staining of neutral lipids and quantification of cellular triacylglycerol content in skin fibroblasts. (**a**) BODIPY staining of neutral lipids in skin fibroblasts from control (Ctrl B) and two LMS patients (Pat. 1, P269S and Pat. 4, Q353R). Two representative confocal images (objectif 60X) per cell line are shown. Neutral lipids were stained with BODIPY 493/503, nuclei were stained with DAPI (blue). Scale bar, 20 μm. Lipid droplets (containing stored neutral lipids, such as triacylglycerols and cholesteryl esters) show punctate BODIPY staining, while the diffuse green staining is likely displayed by reticulate structures of the cell. (**b**) average BODIPY intensity in arbitrary fluorescence units (AFU) from 5 random fields/cell line, containing >15 cells each (**c**) Cellular triacylglycerol (TAG) content of skin fibroblasts from control (Ctrl B) and two LMS patients (P269S and Q353R). Data are means ± S.D. of triplicate analyses.

Supplementary Figure 11 – Quantitative analysis of "apoptosis" rate (Annexin V positive / total cells) was applied to three controls and three LMS cell lines. Bars indicate means±SEM. A 6-fold increase in number of Annexin V positive cells was observed in LMS fibroblasts (*P<0,05).
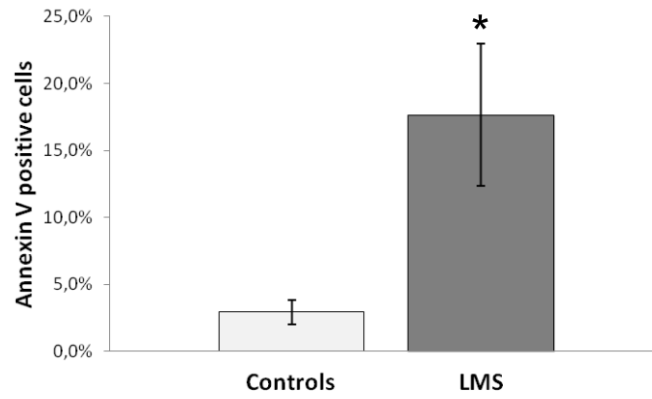
References

1. Saraiva, J. M. Dysgenesis of corpus callosum in Lenz-Majewski hyperostotic dwarfism. *American journal of medical genetics* **91,** 198–200 (2000).

2. Wattanasirichaigoon, D., Visudtibhan, A., Jaovisidha, S., Laothamatas, J. & Chunharas, A. Expanding the phenotypic spectrum of Lenz-Majewski syndrome: facial palsy, cleft palate and hydrocephalus. *Clinical Dysmorphology* **13,** 137–142 (2004).

3. Chrzanowska, K. H., Fryns, J. P., Krajewska-Walasek, M., Van den Berghe, H. & Wisniewski, L. Skeletal dysplasia syndrome with progeroid appearance, characteristic facial and limb anomalies, multiple synostoses, and distinct skeletal changes: a variant example of the Lenz-Majewski syndrome. *American journal of medical genetics* **32,** 470–4 (1989).

4. Majewski, F. Lenz-Majewski hyperostotic dwarfism: reexamination of the original patient. *American journal of medical genetics* **93,** 335–8 (2000).

5. Gorlin, R. J., Whitley, C. B., Gorlin, J. & Ph, D. Lenz-Majewski syndrome. *Radiology* **149,** 129–31 (1983).

6. Robinow, M., Johanson, A. J. & Smith, T. H. The Lenz-Majewski hyperostotic dwarfism. A syndrome of multiple congenital anomalies, mental retardation, and progressive skeletal sclerosis. *The Journal of pediatrics* **91,** 417–21 (1977).

7. Lenz, W. D. & Majewski, F. A generalized disorders of the connective tissues with progeria, choanal atresia, symphalangism, hypoplasia of dentine and craniodiaphyseal hypostosis. *Birth defects original article series* **10,** 133–6 (1974).

8. Kaye, C. I., Fisher, D. E. & Esterly, N. B. Cutis laxa, skeletal anomalies, and ambiguous genitalia. *American journal of diseases of children (1960)* **127,** 115–7 (1974).

9. Macpherson, R. I. Craniodiaphyseal dysplasia, a disease or group of diseases? *Journal of the Canadian Association of Radiologists* **25,** 22–33 (1974).

10. Braham, R. L. Multiple congenital abnormalities with diaphyseal dysplasia (Camurati-Engelmann's syndrome). Report of a case. *Oral surgery, oral medicine, and oral pathology* **27,** 20–6 (1969).

11. Toriello, H. V & Meck, J. M. Statement on guidance for genetic counseling in advanced paternal age. *Genetics in medicine : official journal of the American College of Medical Genetics* **10,** 457–60 (2008).

12. Nishimura, G., Harigaya, a, Kuwashima, M. & Kuwashima, S. Craniotubular dysplasia with severe postnatal growth retardation, mental retardation, ectodermal dysplasia, and loose skin: Lenz-Majewski-like syndrome. *American journal of medical genetics* **71,** 87–92 (1997).

13. Dateki, S. *et al.* A Japanese patient with a mild Lenz-Majewski syndrome. *Journal of human genetics* **52,** 686–9 (2007).

14. Adzhubei, I. A. *et al.* A method and server for predicting damaging missense mutations. *Nature methods* **7,** 248–9 (2010).

15. Sherry, S. T. *et al.* dbSNP: the NCBI database of genetic variation. *Nucleic acids research* **29,** 308–11 (2001).

16. The 1000 Genomes Project Consortium. A map of human genome variation from population-scale sequencing. *Nature* **467,** 1061–73 (2010).

17. Ng, P. C. & Henikoff, S. Predicting deleterious amino acid substitutions. *Genome research* **11,** 863–74 (2001).

18. Choi, Y., Sims, G. E., Murphy, S., Miller, J. R. & Chan, A. P. Predicting the functional effect of amino acid substitutions and indels. *PloS one* **7,** e46688 (2012).

19. Li, B. *et al.* Automated inference of molecular mechanisms of disease from amino acid substitutions. *Bioinformatics (Oxford, England)* **25,** 2744–50 (2009).

20. Larkin, M. a *et al.* Clustal W and Clustal X version 2.0. *Bioinformatics (Oxford, England)* **23,** 2947–8 (2007).

21.   Bligh, E. G. & Dyer, W. J. A rapid method of total lipid extraction and purification. *Canadian journal of biochemistry and physiology* **37,** 911–7 (1959).

22.   Trabzuni, D. *et al.* MAPT expression and splicing is differentially regulated by brain region: relation to genotype and implication for tauopathies. *Human molecular genetics* **21,** 4094–103 (2012).

23.   Trabzuni, D. *et al.* Quality control parameters on a large dataset of regionally dissected human control brains for whole genome expression studies. *Journal of neurochemistry* **119,** 275–82 (2011).

24.   Kang, H. J. *et al.* Spatio-temporal transcriptome of the human brain. *Nature* **478,** 483–9 (2011).